



Implications of particle size on the respective solid-state properties of naltrexone in PLGA microparticles

Andrew Otte^{a,*}, Hazal Turasan^a, Kinam Park^{a,b,c}

^a Purdue University, Weldon School of Biomedical Engineering, West Lafayette, IN 47907, USA

^b Purdue University, College of Pharmacy, West Lafayette, IN 47907, USA

^c Akina, Inc., West Lafayette, IN 47906, USA

ARTICLE INFO

Keywords:

PLGA microparticles
Naltrexone
Crystallinity
Drug release

ABSTRACT

A thorough understanding of the complexities in formulating and manufacturing polymeric microspheres is required for new and generic drug applications. Specifically, for an ANDA application for polymeric microsphere-based products, the applicant must meet Q1 (qualitative) and Q2 (quantitative) sameness, and in some cases, Q3 (e.g., microstructural) sameness. Herein, we report the naltrexone crystallinity in a PLGA microparticle system prepared from a dichloromethane-benzyl alcohol solvent system results in a crystallinity dependence as a function of microparticle size from the same batch – illustrating intrabatch microstructural variability. As the particle size increases, the crystallinity increases, with additional polymorphic forms more readily noted at the large particle sizes. Furthermore, during dissolution, a polymorphic transition and/or crystallization occurs at larger size fractions. This study highlights the importance of controlling the manufacturing parameters during microparticle formation, specifically solvent extraction and particle size control. Furthermore, with the approval of generic microparticles formulations on the horizon, this study highlights the importance of Q3, *the same components in the same concentration with the same arrangement of matter*, whereby microparticles can have varying microstructural properties across particle sizes from the same batch.

1. Introduction

PLGA based microparticle systems have many well-documented advantages relative to other controlled release systems, including complete biodegradability (via lactic acid and glycolic acid), biocompatibility, ease of administration, and long-acting controlled release of various types of therapeutics. Since the approval of Lupron Depot® in 1989, approximately two dozen PLGA-based drug delivery systems have been approved for clinical usage (Park et al., 2021). Although many of them are no longer under patent protection, not a single generic version has been approved by the Food and Drug Administration (FDA). The extraordinary complexity of these types of systems, where manufacturing differences (Garner et al., 2018), variability in the PLGA between sources (Wan et al., 2021), PLGA molecular weight distribution (Ochi et al., 2021), and microparticle size (Chen et al., 2017), among others, have all shown to have significant influences on the *in vitro* and/or *in vivo* kinetics – complicating regulatory aspects. Additionally, a lack of compendial test methods and adequate means of characterizing PLGA can further challenge regulators.

Microparticle size is a relatively simple parameter to characterize and highly influential regarding its impact on release. Increasing particle size subsequently increases the diffusion path length when water imbibes into the system and the respective diffusion outwards. While this is undoubtedly correct, this theory assumes the particle microstructure is the “same” as a function of particle size. At the relative size, microparticles are manufactured and subsequently characterized (i.e., ~5–150 μm); this assumption is likely valid. However, there may be instances where this assumption may not hold. Microparticle properties can be altered by many different manufacturing parameters, such as PLGA characteristics (e.g., lactide:glycolide (L:G) ratio, molecular weight (MW), end group chemistry), and potentially most importantly, drug loading.

Gefitinib microparticles were prepared in acid end-capped 50:50 PLGA in a dichloromethane/dimethyl sulfoxide solvent system (Chen et al., 2017). The drug loading was 6.3% in the microparticles (un-sieved) and varied from 2.4% to 7.6% with increasing size fraction. It is a relatively low drug loading from an amorphous solid dispersion standpoint. Gefitinib was shown to be X-ray amorphous, and only a single T_g

* Corresponding author.

E-mail address: aotte@purdue.edu (A. Otte).

<https://doi.org/10.1016/j.ijpharm.2022.122170>

Received 26 May 2022; Received in revised form 15 August 2022; Accepted 30 August 2022

Available online 5 September 2022

0378-5173/© 2022 Elsevier B.V. All rights reserved.

was observed (by DSC) for all the size fractions, indicating it is likely and/or predominately molecularly dispersed in the PLGA matrix. The rapid release was observed for microparticles less than 50 μm , whereas larger particles illustrated a sigmoidal to zero type release pattern. Gasmí *et al.*, showed that, in a dexamethasone-PLGA 50:50 system, crystallinity was detected via PXRD once the drug loading reached $\sim 30\%$ (Gasmí *et al.*, 2016). The drug release was significantly impacted by loading, where a burst was seen at loadings of $\sim 30\%$, and higher and sigmoidal release with no burst was observed for loadings less than $\sim 20\%$. In the lidocaine-PLGA 50:50 system, the release rate decreased with increasing microparticle size (Klose *et al.*, 2006). No crystallinity was detected in this system via DSC and SEM, although the drug loading was only $\sim 4\%$.

This manuscript aims to delineate the potential implications that particle size can have on the solid-state properties of naltrexone in PLGA microparticles. The three small molecules incorporated into FDA-approved long-acting injectable PLGA microparticle systems are naltrexone, risperidone, and triamcinolone acetonide, with loadings of 33.7% [8], 38.1% [9], and 25% [10], respectively. While low drug loadings can be advantageous in characterizing the polymer microstructure, delineating the impact on clinically relevant drug loadings is equally important. The aim of this manuscript is to report the effect of how the microparticle size can potentially influence the solid-state properties of encapsulated naltrexone in PLGA microparticles, as naltrexone has been demonstrated to crystallize in PLGA microparticles (Brittain *et al.*, 2007; Otte and Park, 2022) (extent and form(s) dependent on formulation and manufacturing parameters). As illustrated in Fig. 1, naltrexone encapsulated into a 75:25 ester end-capped PLGA resulted in microparticles that appeared to increase in birefringence as a function of particle size. Similar to how the tortuosity and pathlength dictate drug release, these same parameters influence the solvent extraction kinetics during microparticle formation. Therefore, it is hypothesized these same parameters may also influence the solid-state properties of the encapsulated drug molecule.

2. Materials

Ester end-capped 75:25 PLGA from Evonik® (Birmingham, Alabama) and naltrexone free base anhydrous from SpecGx, LLC (St. Louis, MO) were used. Dichloromethane (DCM), benzyl alcohol (BA), acetonitrile, methanol, potassium phosphate monobasic, and sodium azide were procured from Fisher Scientific (Fair Lawn, NJ). Emprove® Essential 40–88 (Poly(vinyl alcohol) (PVA)) was obtained from Millipore Sigma (Darmstadt, Germany). Sodium L-ascorbate and phosphate-buffered saline with 0.05 % Tween® 20, pH 7.4 (PBST) were

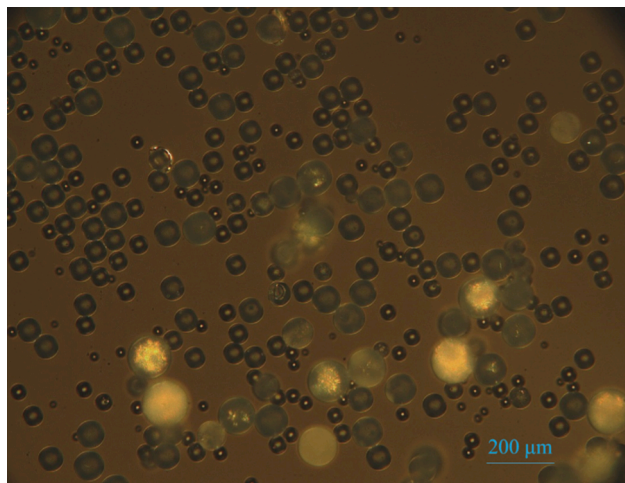


Fig. 1. A polarized light microscopy image of naltrexone-PLGA microparticles.

purchased from Sigma Aldrich (St. Louis, MO).

3. Methods

3.1. Preparation of naltrexone microparticles

The organic phase consisted of PLGA 75:25 (RG 756S) and naltrexone (free base) dissolved in DCM and BA. The naltrexone mixing was kept to less than 15 min to minimize the degradation of PLGA. An in-line mixing assembly was fit onto a Silverson L5M-A homogenizer to convert it into an in-line homogenizer. The continuous phase, 1% PVA in ultrapure water, and discontinuous phase, PLGA and NTX dissolved in DCM and BA, were pumped through a Cole-Parmer gear pump and syringe pump at 300 mL/min and 100 mL/min, respectively, with a target batch size of 25 g or 250 g (10X volumes for extraction and ethanol wash). The two phases were pumped into the homogenizer via a tube-in-tube design to minimize any premixing of the two phases prior to homogenization. Homogenization was performed at 1800 RPM with a medium emulsor screen. Subsequently, the phases were transferred directly into the extraction vessel loaded with 15.2 L of water at 4 °C and hardened for 4 h. The hardened microparticles were collected and dewatered on a 25 μm sieve mesh. Microparticles were further hardened overnight in a vacuum oven for 18 h and washed with 4 L of 25% ethanolic solution at 22 °C for 8 h. Post-extraction, microparticles were collected between 25 and 150 μm , dewatered, and dried under vacuum for 48 h.

3.2. Characterization of naltrexone microparticles

1. High-performance liquid chromatography

Naltrexone quantitation was performed with an Agilent 1260 HPLC system with a UV absorbance detector. The HPLC had the following conditions: Mobile Phase: 65:35 methanol:potassium phosphate buffer, pH 6.6; flow rate: 1.0 mL/min; autosampler temperature: room temperature; column temperature: 30 °C; detection: 210 nm (UV); total run time: 7 min; injection volume: 2.5 μL (drug loading) 10 μL (*in vitro* release); column: Zorbax SB-C18 150 \times 4.6 mm, 5 μm ; and approximate retention time of naltrexone: 4.8 min. The lower injection volume for drug loading was used to minimize the volume of PLGA injected into the HPLC column.

2. Drug Loading and Benzyl Alcohol Content

Approximately 5–7 mg of the various samples was weighed, dissolved in 5 mL of acetonitrile, and subsequently diluted with the mobile phase. 2.5 μL was then injected with the same HPLC conditions as the *in vitro* release samples.

3. *In vitro* drug release

20 mL of pH 7.4 phosphate-buffered saline with 0.05% Tween 20 (PBST) and 0.0625% (w/v) sodium ascorbate and 5–7 mg of microparticles were placed in a stoppered 50 mL Erlenmeyer flask and placed in a 37.0 °C (± 0.3 °C) glycerol baths at 30 RPM in a shaking incubator. 1 mL aliquots were taken at various time points throughout the study and replaced with a fresh release medium. Naltrexone content in the release medium was analyzed via HPLC.

4. Imaging

The morphology of various lots was characterized with a Tescan Vega 3 scanning electron microscope. Microparticles were mounted onto carbon taped aluminum stubs and sputter-coated with a gold–palladium mixture under vacuum in the presence of argon.

5. Powder X-ray diffraction

Powder diffraction (PXRD) data were collected on a Panalytical Empyrean X-ray diffractometer equipped with Bragg-Brentano HD optics, a sealed tube copper X-ray source ($\lambda = 1.54178 \text{ \AA}$), soller slits on both the incident and receiving optics sides, and a PixCel3D Medipix detector. Samples were packed in metal sample cups with a 16 mm wide and 2 mm deep sample area. anti-scatter slits and divergence slits, as well as masks, were chosen based on sample area and starting θ angle. Data were collected between 4 and 35° in 2θ using the Panalytical Data Collector software.

The influence of incubation time on crystallinity experiments was performed with the same concentration of naltrexone microparticles in PBST as the *in vitro* drug release for the 250 g batch sample. As the representative PXRD patterns exhibited similar forms across the sieve fractions, only this sample was utilized in this portion of the study based on the material available. Samples were collected on a Buchner funnel on filter paper and “dried” for 10 min to remove excess/surface PBST, then analyzed via PXRD and residual water content.

6. Particle Size Distribution

The particle size distribution was measured using a CILAS 1190 particle size analyzer (Madison, WI). Approximately 50 mg of microspheres were dispersed in 1.5 mL of a 0.1% Tween 80 aqueous solution and subsequently analyzed. The particle size distributions were measured in triplicate.

7. Residual Water Content

A Mettler Toledo V10S compact volumetric Karl Fischer Titrator was used to determine the water content. A 3:1 chloroform:methanol solution was used as the solvent. Between 15 and 25 mg of microparticles was used for the analysis, and each sample was performed in triplicate. A sodium tartrate dihydrate standard was used as a reference material.

8. Statistical Data Analysis

All data are presented as means with standard deviation (SD). Statistical analyses were performed using Prism 9.0 (GraphPad Software, La Jolla, CA) using unpaired t-tests at significance levels of $P < 0.05$.

4. Results and discussion

Minor alterations in the manufacturing process have resulted in differences in the resultant microparticle properties. The results of this study are being highlighted to demonstrate the properties of microparticles, specifically the release, and most notably, the solid-state properties of the drug encapsulated in the matrix can vary across the particle size distribution in a single batch.

Fig. 2 shows the measured particle size distribution of the two batches of naltrexone-PLGA microparticles. The size distributions are similar as they were collected between 25 and 150 μm sieves. A larger number of fines ($<25 \mu\text{m}$) were observed in the 250 g batch, which skews the distribution relative to the 25 g batch ($6.86 \pm 0.83\%$ vs $4.49 \pm 0.40\%$, respectively). This skew is likely due to incomplete sieving and/or sieves that become clogged due to the larger quantity of microparticles. Table 1. highlights the data of the three sieve cuts used for the distribution of 25–53, 53–106, and 106–150 μm . No statistical difference was found between the sieve cuts of the two batches. Tables 2 and 3 illustrate the drug loadings of the full batches and various sieve cuts of the two batches. The 25 g batch has slightly higher drug loadings than the 250 g, potentially due to the lower residual BA contents.

The representative images of the various sieve cuts are shown in Fig. 3. The 3 sieved cuts of the 25 g batch appear to show the particles are mostly spherical without any significant surface features to note. The

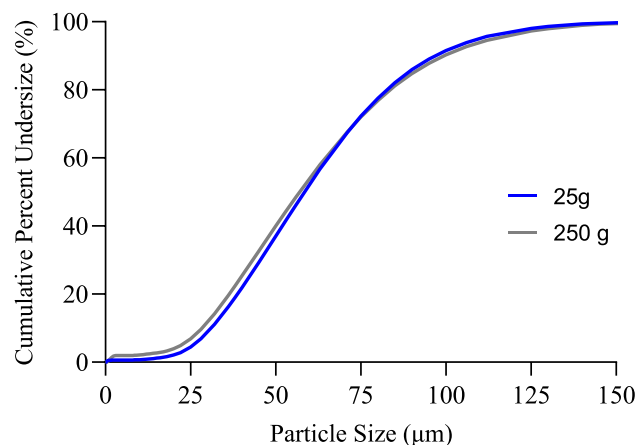


Fig. 2. Microparticle size distribution of the 25 and 250 g batches.

Table 1

Volume percent (%) of particles in the three sieve fractions. (no statistical difference between intrabatch sieve cuts).

Batch	$<53 \mu\text{m}$	$53\text{--}106 \mu\text{m}$	$106\text{--}150 \mu\text{m}$
25 g	41.71 ± 4.73	52.2 ± 1.26	6.09 ± 3.61
250 g	44.39 ± 4.02	48.29 ± 2.71	7.31 ± 1.48

Table 2

Naltrexone loading (%) as a function of size fraction. (no statistical difference between intrabatch sieve cuts, with * showing interbatch statistical difference).

Batch	Full Batch	$<53 \mu\text{m}$	$53\text{--}106 \mu\text{m}$	$106\text{--}150 \mu\text{m}$
25 g	36.2 ± 0.5	36.4 ± 0.8	36.7 ± 0.3	35.7 ± 0.5
250 g	$35.2 \pm 0.3^*$	35.4 ± 0.8	$35.1 \pm 0.3^*$	35.2 ± 0.4

Table 3

Residual benzyl alcohol (%) as a function of size fraction. (each intra and interbatch sieve cut is statistically different than the other).

Batch	Full Batch	$<53 \mu\text{m}$	$53\text{--}106 \mu\text{m}$	$106\text{--}150 \mu\text{m}$
25 g	1.52 ± 0.00	0.99 ± 0.02	1.65 ± 0.02	2.51 ± 0.09
250 g	1.81 ± 0.01	1.24 ± 0.03	1.91 ± 0.02	2.34 ± 0.03

250 g batch seems to have a large quantity of particles exhibiting a wrinkled morphology, particularly in the 53–106 μm cut, along with some particles showing buckles in the surface (Park et al., 2021). In this study, the 250 g scale is prepared by allowing the continuous and discontinuous phases to run for a longer duration into a volume 10X the 25 g scale. While the solvent extraction conditions are similar across the two scales during the formation of the seed emulsion phase, the 250 g batch flows into a volume 10X that the 25 g batch. Therefore, as the seed emulsion flows into the extraction tank, the initial seed emulsion from the 250 g batch sees a greater concentration gradient relative to the 25 g batch due to the volume difference. This could result in a difference between the shell formation kinetics between the two scales, ultimately impacting the overall solvent extraction kinetics and morphology (Park et al., 2019). This could be one possibility for the slight difference in morphology.

Fig. 4 illustrates the drug release as a function of batch size and sieve cuts between the two batches. The drug release curves all appear to be tri-phasic, with a clear dependency on particle size. As expected, as the size of sieve cut increases, the naltrexone release rate decreases. Since the drug loadings are similar across the sieve cuts from each respective batch, the release kinetics are likely due to the microparticle size, respective drug-polymer microstructure, and/or naltrexone

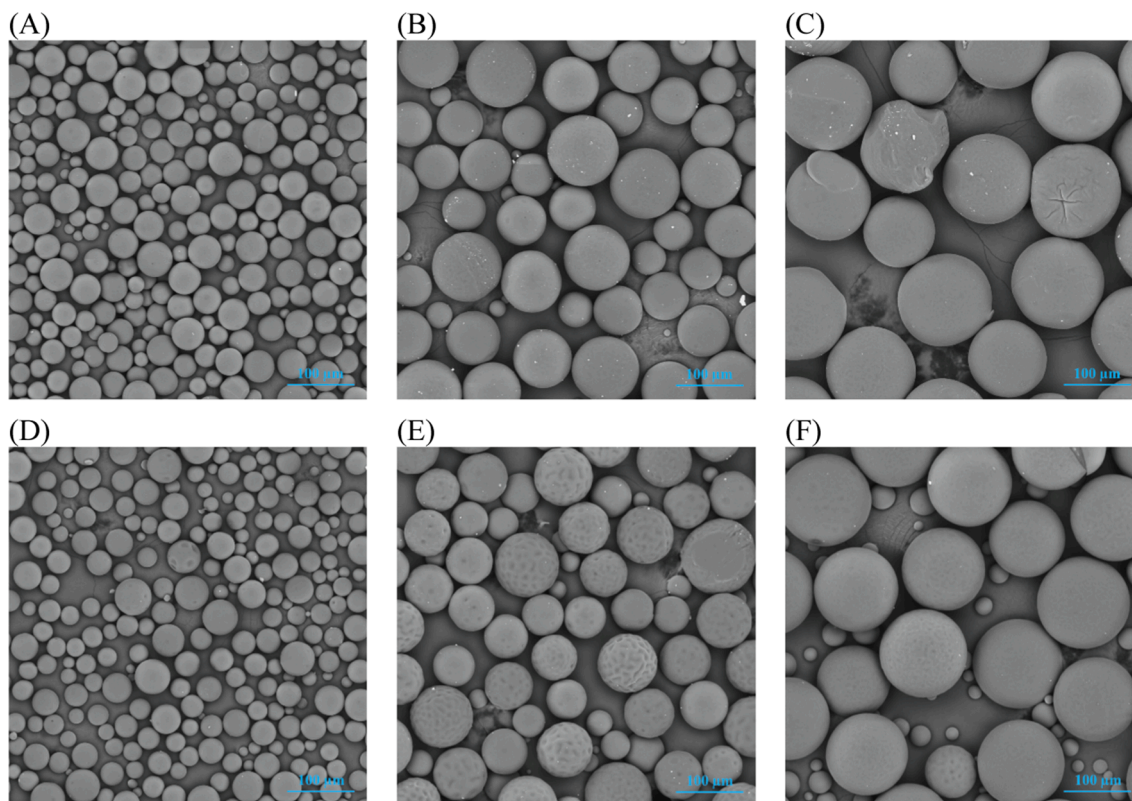


Fig. 3. SEM images of sieve cuts (A) 25–53 μm , (B) 53–106 μm , and (C) 106–150 μm for the 25 g batch and (D) 25–53 μm , (E) 53–106 μm , and (F) 106–150 μm for the 250 g batch.

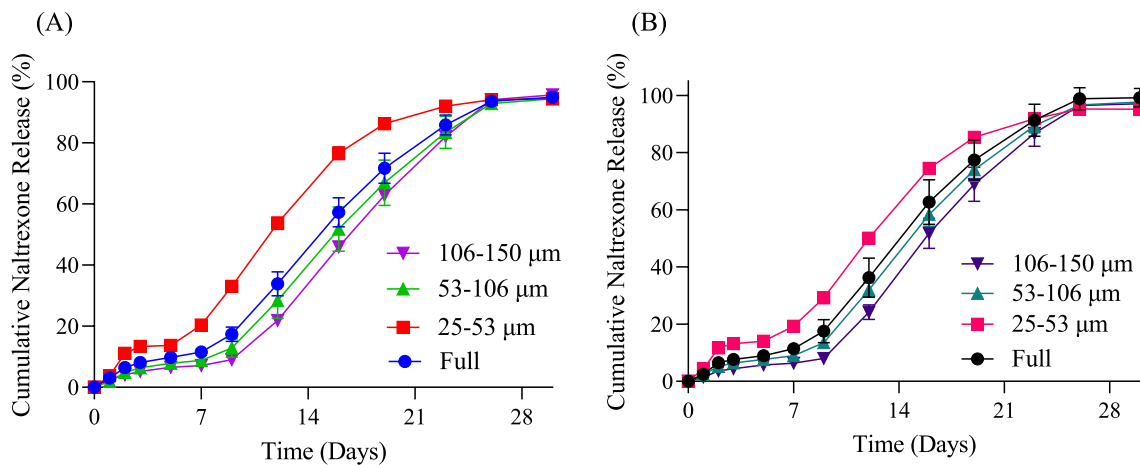


Fig. 4. *In vitro* naltrexone release as a function of particle size from the 25 g (A) and 250 g (B) batches.

crystallinity.

Fig. 5 illustrates the X-ray diffraction patterns of the full batches compared to the respective sieved fractions. The diffraction patterns show the crystallinity is dependent on microparticle size. Again, the drug loading is similar across the sieve cuts from each separate batch; therefore, the crystallinity is not a function of the drug loading. Varying the solvent type/ratio can impact the inner structure of the microparticles via the distribution of polymeric molecules and the formation of the core-shell structure (Xiao et al., 2013). Furthermore, the rate of solvent diffusion and subsequent microparticle solidification can impact both the shell formation and microstructure.

Few models exist for solidification, but the modeling generally consists of Fick's law of solvent diffusion in the droplet coupled with

boundary layer and droplet shrinkage calculations (Li et al., 2008). In general, smaller microparticles will have a faster extraction rate due to the high surface area, resulting in a higher concentration of solvent in the continuous phase and subsequent extraction phase. This fast solvent extraction rate is more likely to lead to an amorphous dispersion due to a lack of time for phase segregation/mobility, ultimately leading to crystallization if given/observed over a significant time frame (Brough and Williams, 2013; Izumikawa et al., 1991). The system being characterized is formulated from a co-solvent system of DCM/BA, further adding to the complexity due to boiling point (39.6 vs 205 $^{\circ}\text{C}$) and aqueous solubility (1.37–2.0 vs 3.5–4.3 g/L at 20 $^{\circ}\text{C}$ (Mackay, 2006)) differences between the two solvents. Finally, an intermediate drying step and an ethanol wash are utilized to further remove residual solvent. The

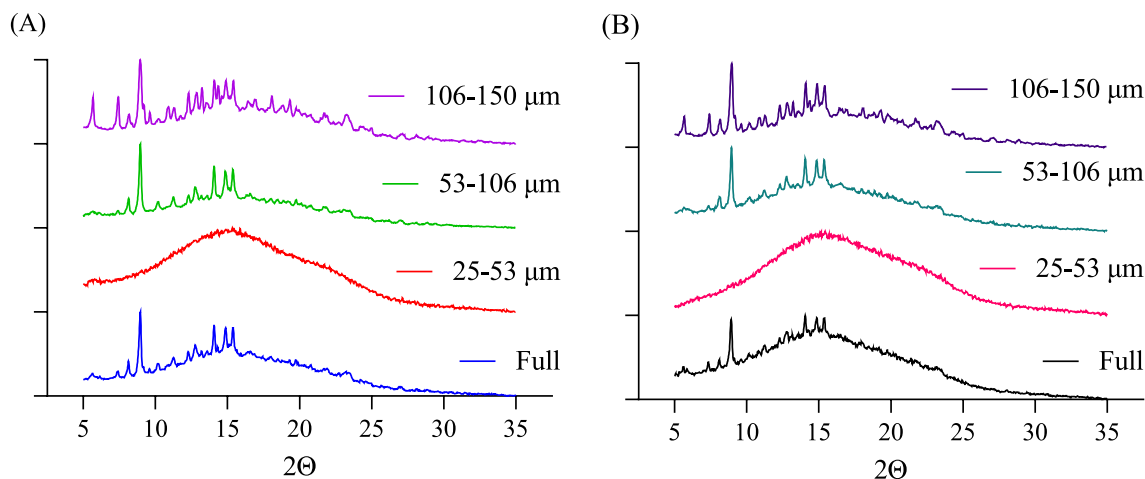


Fig. 5. PXRD patterns of the full batch and sieve cuts – 25 g (A) and 250 g (B) batch.

impacts of these steps and the potential ramifications on the crystallinity/polymorphism and polymer microstructure as a function of microparticle size have not been fully elucidated to date.

It is hypothesized that intermediate drying removes residual solvent (in this instance, DCM) and allows structural relaxation of the polymer, increasing molecular density. During the ethanolic wash, this further removes DCM and BA. If the domain size of naltrexone is a sufficient size during this step, it may result in (further) crystallization depending on the kinetics. Furthermore, an additional polymorphic form(s) of naltrexone is more readily noted in the 106–150 μm fraction relative to the 53–106 μm fraction as noted by the diffraction peaks at ~ 5.7 and $\sim 7.4^\circ 2\theta$.

Hua *et al.*, performed a reverse engineering process on Vivitrol® using ethyl acetate and BA system and demonstrated similarity in quality attributes and *in vitro* release (Hua *et al.*, 2021). Although, the crystallinity of naltrexone was not disclosed. An dhariya *et al.*, produced three compositionally equivalent formulations of naltrexone microspheres with different release characteristics and manufacturing techniques, ultimately establishing and validating an IVIVC (An dhariya *et al.*, 2017). A continuous in-line approach produced naltrexone-loaded PLGA microparticles with reproducible size distributions, drug loadings, and release rates (Sharifi *et al.*, 2020). Neither of these publications disclosed the resultant crystallinity of naltrexone. Therefore, if the described crystallinity results here are a function of this formulation and/or manufacturing technique, it requires further exploration and its impacts on the stability and the *in vivo* performance.

PBST imbibing into the microparticle could impact the naltrexone crystallinity over time. PBST induction experiments were performed under the same sink conditions as the *in vitro* drug release experiments to mimic potential *in vivo* conditions. Localized drug concentrations in the microparticle could be substantially above the naltrexone solubility limit, potentially leading to favorable crystallization conditions – particularly at *in vivo* temperature conditions ($\sim 37^\circ\text{C}$.) Fig. 6 illustrates the PXRD patterns as a function of time, with Fig. 7 showing the respective water contents at said time points. The $<53\ \mu\text{m}$ fraction samples remain X-ray amorphous over time, reaching $\sim 80\%$ water content at 72 h. A large amount of water grossly distorts the amorphous halo of the naltrexone-PLGA mixture. A tiny peak may be present at $\sim 10.9^\circ 2\theta$ at 24 and 48 hrs, although this is readily debatable whether it is background noise or due to the presence of crystallinity. For the 53–106 μm fraction, the PXRD pattern changes as a function of time, where there appears to be a crystallization event and/or a polymorphic transition during water uptake. The peak at $\sim 9.0^\circ 2\theta$ decreases in intensity over time, whereas the peak at $\sim 10.9^\circ 2\theta$ begins to appear at 4 hrs and reaches maximum intensity at 48 hrs. In this sample, the water content begins to distort the pattern at 72 hrs, although diffraction peaks

are still visible between $5\text{--}20^\circ 2\theta$. Crystallinity appears to be mostly absent by day 7. For the 106–150 μm fraction, the peak at $\sim 9.0^\circ 2\theta$ also appears to decrease in intensity over time, although the increase in the peak at $\sim 10.9^\circ 2\theta$ in the 53–106 μm fraction is not as readily noted in the 106–150 μm fraction. As expected, the water uptake for this fraction proceeds at the slowest rate. It reaches $\sim 75\%$ at day 7, coinciding with the absence of crystallinity of naltrexone and a similar PXRD amorphous halo to that of the 53–106 μm sample.

This particle size-crystallinity dependence is likely a continuum over the microparticle size range characterized. Ten crystal structures of naltrexone have been disclosed to date (2022), with additional multiple forms being disclosed without representative structures (Brittain *et al.*, 2007). According to US Patent 7,279,579 B2, naltrexone exists in four different forms in a PLGA microsphere prepared from an ethyl acetate-BA mixture via a static mixing approach, intermediate drying, and ethanolic wash. Additionally, the ratio of these forms was described as influencing the *in vitro* release rate (Brittain *et al.*, 2007). Although, whether there is a propensity for these forms to vary across microparticle size was not disclosed.

To further explore the crystallinity of the size fractions, the BA solvate and ethanolate forms were prepared according to (Brittain *et al.*, 2007), the diffraction data for the monohydrate form data was obtained from the CCDC database [YIGRAI – 643261], and the anhydrous free base is as received from the supplier. The peak at $9.0^\circ 2\theta$ appears to coincide with the ethanolate form in both the 53–106 and 106–150 μm fractions (Fig. 8.). The benzyl alcohol solvate form, identified by the $5.7^\circ 2\theta$ peak, appears to be mostly devoid in the 53–106 μm fraction, whereas it is substantially present in the 106–150 μm fraction. In both fractions, particularly the 53–106 μm fraction, the increasing intensity of the $10.9^\circ 2\theta$ peak potentially corresponding to the anhydrous form is readily apparent. This potential anhydrous form could result from a dehydration/solvation event or crystallization from amorphous content in the microparticle. Many structural and solid-state changes are occurring in localized micron and sub-micron regions in the microparticle, further illustrating the complexity of these systems, both during manufacturing and usage.

5. Conclusion

The increase in crystallinity as a function of size is hypothesized to be due to a combination of manufacturing variables, most notably the solvent extraction kinetics and post-treatment methods. Similar to how the tortuosity and path length dictate drug release, these same parameters are also likely influential on the solvent extraction kinetics during microparticle formation. They can result in varying localized regions of inhomogeneity in the microparticles leading to preferential

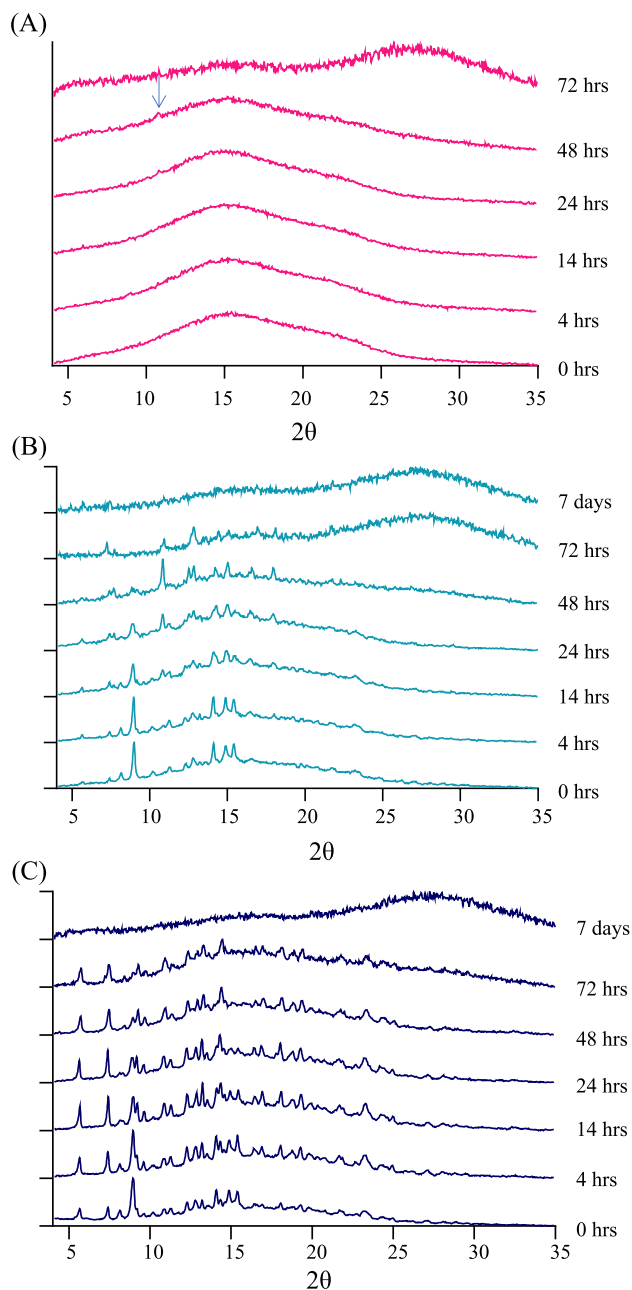


Fig. 6. PXRD patterns of sieve cut samples after exposure to PBST at 37 °C (A) 25–53 (B) 53–106, and (C) 106–150 µm for the 250 g batch.

crystallization. Here we report that naltrexone can both crystallize in the polymer matrix and crystallize into different polymorphic forms based on the size of the PLGA microparticle. As has been previously shown, the drug release rate of naltrexone is dependent on microparticle size. However, the exact contributions of the amorphous vs crystalline form have not been explicitly elucidated here. As naltrexone can crystallize into multiple polymorphic forms, future studies will look into the various specific forms coupled with their respective solubility, dissolution, and stability characteristics. This study highlights that the microstructure/microstructural properties may not be equivalent across microparticle sizes from a single batch, adding additional potential complexities to demonstrating Q3 sameness and/or producing generic LAI products that are Q1/Q2/Q3 similar. The analysis described in this manuscript may help develop potential generic naltrexone formulations and other long-acting PLGA-based formulations.

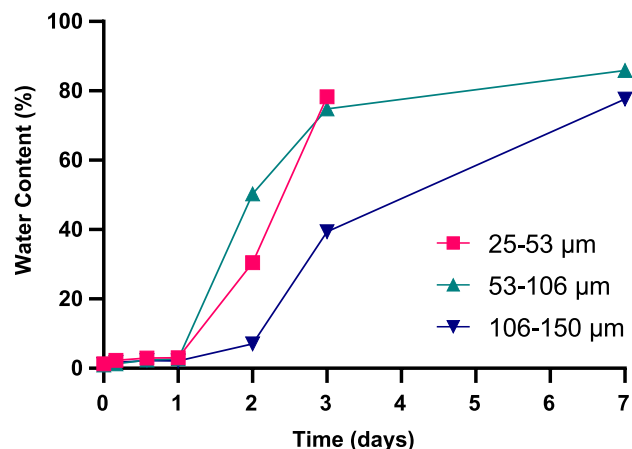


Fig. 7. Water content over time of the three sieve fractions from the 250 g batch.

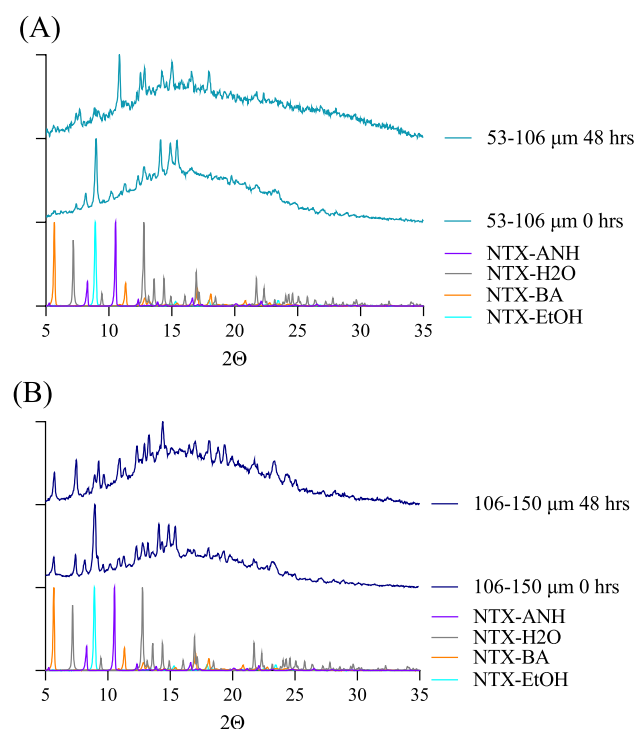


Fig. 8. Naltrexone polymorphic forms compared to the 53–106 (A) and 106–150 µm (B) sieve fractions.

CRediT authorship contribution statement

Andrew Otte: Conceptualization, Investigation, Formal analysis, Data curation, Writing – original draft, Writing – review & editing, Funding acquisition. **Hazal Turasan:** Conceptualization, Investigation, Formal analysis, Data curation, Writing – original draft, Writing – review & editing. **Kinam Park:** Conceptualization, Investigation, Formal analysis, Data curation, Writing – original draft, Writing – review & editing, Supervision, Project administration, Funding acquisition.

Declaration of Competing Interest

The authors declare that they have no known competing financial interests or personal relationships that could have appeared to influence the work reported in this paper.

Data availability

Data will be made available on request.

Acknowledgements

This study was supported by the grant UG3 DA048774 from the National Institute of Drug Abuse (NIDA), the Chong Kun Dang Pharmaceutical Corp., and the Ralph W. and Grace M. Showalter Research Trust Fund.

References

- Andhariya, J.V., Shen, J., Choi, S., Wang, Y., Zou, Y., Burgess, D.J., 2017. Development of in vitro-in vivo correlation of parenteral naltrexone loaded polymeric microspheres. *J. Control. Release* 255, 27–35.
- Brittain, H.G., Dickason, D.A., Hotz, J., Lyons, S.L., Ramstack, J.M., Wright, S.G., 2007. Polymorphic forms of naltrexone. Alkermes Pharma Ireland Ltd.
- Brough, C., Williams, R.O., 2013. Amorphous solid dispersions and nano-crystal technologies for poorly water-soluble drug delivery. *Int. J. Pharm.* 453, 157–166.
2. Cambridge Crystallographic Data Centre, <https://www.ccdc.cam.ac.uk/>.
- Chen, W., Palazzo, A., Hennink, W.E., Kok, R.J., 2017. Effect of Particle Size on Drug Loading and Release Kinetics of Gefitinib-Loaded PLGA Microspheres. *Mol. Pharm.* 14, 459–467.
- Garner, J., Skidmore, S., Park, H., Park, K., Choi, S., Wang, Y., 2018. Beyond Q1/Q2: The Impact of Manufacturing Conditions and Test Methods on Drug Release From PLGA-Based Microparticle Depot Formulations. *J. Pharm. Sci.* 107, 353–361.
- Gasmi, H., Siepmann, F., Hamoudi, M.C., Danede, F., Verin, J., Willart, J.F., Siepmann, J., 2016. Towards a better understanding of the different release phases from PLGA microparticles: Dexamethasone-loaded systems. *Int. J. Pharm.* 514, 189–199.
- Hua, Y., Wang, Z., Wang, D., Lin, X., Liu, B., Zhang, H., Gao, J., Zheng, A., 2021. Key Factor Study for Generic Long-Acting PLGA Microspheres Based on a Reverse Engineering of Vivitrol®. *Molecules* 26, 1247.
- Izumikawa, S., Yoshioka, S., Aso, Y., Takeda, Y., 1991. Preparation of poly(L-lactide) microspheres of different crystalline morphology and effect of crystalline morphology on drug release rate. *J. Control. Release* 15, 133–140.
- Klose, D., Siepmann, F., Elkharraz, K., Krenzlin, S., Siepmann, J., 2006. How porosity and size affect the drug release mechanisms from PLGA-based microparticles. *Int. J. Pharm.* 314, 198–206.
- Li, M., Rouaud, O., Poncelet, D., 2008. Microencapsulation by solvent evaporation: State of the art for process engineering approaches. *Int. J. Pharm.* 363, 26–39.
- Mackay, D., 2006. Handbook of physical-chemical properties and environmental fate for organic chemicals, 2nd ed. CRC/Taylor & Francis, Boca Raton, FL.
- Ochi, M., Wan, B., Bao, Q., Burgess, D.J., 2021. Influence of PLGA molecular weight distribution on leuprolide release from microspheres. *Int. J. Pharm.* 599, 120450.
- Otte, A., Park, K., 2022. Transitioning from a lab-scale PLGA microparticle formulation to pilot-scale manufacturing. *J. Control. Release* 348, 841–848.
- Park, K., Skidmore, S., Hadar, J., Garner, J., Park, H., Otte, A., Soh, B.K., Yoon, G., Yu, D., Yun, Y., Lee, B.K., Jiang, X., Wang, Y., 2019. Injectable, long-acting PLGA formulations: Analyzing PLGA and understanding microparticle formation. *J. Control. Release* 304, 125–134.
- Park, K., Otte, A., Sharifi, F., Garner, J., Skidmore, S., Park, H., Jhon, Y.K., Qin, B., Wang, Y., 2021. Formulation composition, manufacturing process, and characterization of poly(lactide-co-glycolide) microparticles. *J. Control. Release* 329, 1150–1161.
- Sharifi, F., Otte, A., Yoon, G., Park, K., 2020. Continuous in-line homogenization process for scale-up production of naltrexone-loaded PLGA microparticles. *J. Control. Release* 325, 347–358.
- Wan, B., Bao, Q., Zou, Y., Wang, Y., Burgess, D.J., 2021. Effect of polymer source variation on the properties and performance of risperidone microspheres. *Int. J. Pharm.* 610, 121265.
- Xiao, C.-D., Shen, X.-C., Tao, L., 2013. Modified emulsion solvent evaporation method for fabricating core-shell microspheres. *Int. J. Pharm.* 452, 227–232.